IEEE Access
Multidisciplinary | Rapid Review | Open Access Journal

Received March 15, 2019, accepted March 29, 2019, date of publication April 9, 2019, date of current version April 19, 2019.

Digital Object Identifier 10.1109/ACCESS.2019.2909816

Optimal Setting and Control Strategy for Industrial Process Based on Discrete-Time Fractional-Order PI$^{\lambda}$D$^{\mu}$

FENGXUE ZHANG, CHUNHUA YANG, (Member, IEEE), XIAOJUN ZHOU, AND WEIHUA GUI, (Member, IEEE)
School of Automation, Central South University, Changsha 410083, China

Corresponding author: Xiaojun Zhou (michael.x.zhou@csu.edu.cn)

This work was supported in part by the National Natural Science Foundation of China under Grant 61533021, Grant 61873285, and Grant 61621062, in part by the Innovation-Driven Plan in Central South University under Grant 2018CX012, in part by the Hunan Provincial Natural Science Foundation of China under Grant 2018JJ3683, in part by the Hunan Provincial Innovation Foundation for Postgraduate under Grant CX2018B062, and in part by the financial support from the China Scholarship Council under Grant 201806370157.

ABSTRACT Generally, the main task of the optimal operation in the industrial process is to satisfy the process technical requirements, and the PID controller is a well-known controller in industrial control applications. Nevertheless, due to the complicated mechanisms and the dynamic characteristics of a complex industrial process, the conventional PID controller fails to provide effective control to such systems. In this paper, we develop a novel discrete-time fractional order PID (DFOPID) control strategy to achieve the technical requirements of the complex industrial process. The proposed work is conducted through a combination of three novel interdependent efforts. First, on the basis of the widely used Tustin operator and its Taylor series, a digital structure of the DFOPID is proposed. Second, in order to solve the stability problem of the complex industrial process, an optimal setting of the approximation function's order (N) and five parameters (λ, μ, K_p, K_i, K_d) is necessary. Hence, an integral time absolute error (ITAE) criterion is applied to convert the optimal setting problem to a nonconvex optimization problem. Finally, a novel intelligent optimization search algorithm called state transition algorithm is employed to carry out the aforementioned design procedure. Furthermore, the performance of the DFOPID control strategy in some practical industrial control systems, including the copper removal process and the electrochemical process of zinc are also investigated.

INDEX TERMS Discrete-time system, PI$^{\lambda}$D$^{\mu}$ control, state transition algorithm, discretization method, complex industrial process.

I. INTRODUCTION

In the past several decades, the main task of the optimal operation in industrial process is to satisfy the process technical requirements. PID controllers achieved high achievements and have undoubtedly been the most widely used controllers in various industrial applications. Due to the simplicity of design and implementation of PID controllers, many researchers hope to improve the performance of these controllers by studying new structures and improving adjustment methods [1]. One of the attempts was the general form of the PID controller proposed by Podlubny for the first time, known as the FOPID or PI$^{\lambda}$D$^{\mu}$ controller [2]. Compared with conventional PID, FOPID has unique characteristics such as low sensitivity to external disturbances, infinite dimension, and memory effect [3]. Hence, there are numerous PI$^{\lambda}$D$^{\mu}$-type controllers proposed in various applications. Saleem et al. [4] presented a robust adaptation mechanism for the orders of a FOPID controller in order to optimally regulate the speed of a permanent magnet direct current motor. Monjie et al. [5] applied the PI$^{\lambda}$D$^{\mu}$ controller to a low pressure flowing water circuit control system. In [6], a fractional-order fuzzy PID controller was applied to the binary distillation column system for controlling the distillate composition. Saptarshi et al. [7] applied the hybrid fuzzy PI$^{\lambda}$D$^{\mu}$ controllers to some oscillatory fractional order processes.

It is obvious that there are many superiorities and applications of the PI$^{\lambda}$D$^{\mu}$-type controllers. Nevertheless, because most industrial system models are dynamically non-linear,

The associate editor coordinating the review of this manuscript and approving it for publication was Dusmanta Kumar Kumar Mohanta.

discrete forms of PI$^{\lambda}$D$^{\mu}$-type controllers are required for adjustment and control. And currently, the discrete-time structure of this type of controller can be obtained using a process of modeling in the form of a linear difference equation (which, of course, corresponds to rational transfer functions in the complex z variable). Piotr et al. [8] applied the variable, discrete-time PI$^{\lambda}$D$^{\mu}$ controller in discrete-time control, which showed new unlimited possibilities of shaping its transient characteristics to preserve the proportional, integral, and differential action. A proposition of how to apply a discrete-time PI$^{\lambda}$D$^{\mu}$ controller to the moving part of an experimental oriented photovoltaic system for controlling the elevation angle was investigated in [9]. Ostalczyk et al. [10] focused on the stability analysis of a closed-loop SISO linear discrete-time system with the variable, discrete-time PI$^{\lambda}$D$^{\mu}$ controller. Koksal et al. [11] proposed the application of a PI$^{\lambda}$D$^{\mu}$ controller to a nonlinear two-mass drive system. Mohamad [12] employed direct and indirect strategies for the process of discretization, and these two different methods are compared through implementing the new form of PI$^{\lambda}$D$^{\mu}$ controllers on a discrete-time system. In addition, we can also get some inspirations from other kinds of studies about nonlinear system control, for example, Aranya et al. [13] presented a time-scale separation redesign for stabilization and performance recovery of nonlinear systems with unmodeled dynamics.

However, one of the most intractable problems that hinders the application of the PI$^{\lambda}$D$^{\mu}$ controller in practice is the adjustment of the controller parameters, which greatly affects the tracking performance and stability of the system. FOPID is a special controller in which integral order and differential order are fraction instead of integer. According to our best knowledge, due to the complexity of the PI$^{\lambda}$D$^{\mu}$ controller, there has been no systematic way to set its fractional order parameters. Hence, the main difficulty of designing PI$^{\lambda}$D$^{\mu}$ is to tune the controller parameters. In this study, the problem of adjusting the parameters is converted into a nonconvex optimization problem based on the ITAE criterion. Then, we adopt an intelligent optimization search algorithm to tune the FOPID controller parameters. Nowadays, there are numerous applications of the optimization method that should be given more attentions. Chai et al. [14] used the improved gradient-based algorithm as the inner solver of the constrained space maneuver vehicles trajectory optimization problem, which can offer the user more flexibility to control the optimization process. In [15], the randomness and fuzziness of the foraging behavior of fruit fly swarm in osphresis phase is described by the normal cloud model, which aims to improve the convergence performance of fruit fly optimization algorithm.

Recently, a novel intelligent optimization search algorithm named state transition algorithm (STA), which was proposed based on the concept of state and state transition, has become quite popular due to its simple structure and efficient global search capability [16]–[20]. It has been shown to outperform many types of evolutionary algorithms and heuristic search algorithms like harmonic search and artificial bee colony in solving many well-known benchmark optimization problems [21]. In addition, the strong adaptability and search capability of STA in global optimization have been tested in several real-world applications [22]–[25]. In [26], a discrete-STA was introduced to the water distribution networks to solve the optimal design problem. A multi-objective-STA was investigated for balancing the operating costs and energy efficiency in the alumina evaporation process [27]. A continuous state transition algorithm was used to resolve the overlapping linear sweep voltammetric peaks in the case of small signals overlapping to a very big one [28]. Furthermore, in [29], STA was introduced to select the optimal continuous PI$^{\lambda}$D$^{\mu}$ parameters, and in addition, the effect of the sample size and objective criterion on the performance of the closed-loop system are studied. Hence, in this paper, the STA is applied to solve the optimal design of a discrete-time PI$^{\lambda}$D$^{\mu}$ controller. The effectiveness of the proposed strategy will be tested by actuating the response of some practical industrial processes, such as copper removal process and zinc electrochemical process. Moreover, we use two other metaheuristic algorithms to compare with STA and investigate their convergence rate and robustness in solving discrete-time PI$^{\lambda}$D$^{\mu}$ controller design problem. However, it is worth noting that one of the main disadvantage of applying the intelligent optimization search algorithm is that the parameter optimization process requires a high computational effort, which makes the optimal setting process difficult to apply online. Especially in the complex industrial processes with many disturbances. Therefore, this method is often operated under offline conditions to obtain optimized set values, and provides reference for the factory operators to realize real-time tracking of the process.

In what follows, the contributions of this paper are summarized: (i) A novel DFOPID control strategy based on the Tustin operator and Taylor series is proposed. (ii) On the basis of the optimization theory and ITAE criterion, the problem of adjusting the parameters is converted into a nonconvex optimization problem. (iii) An intelligent optimization search algorithm called STA is introduced to solve the aforementioned optimization problem, and another three search algorithms are adopted to compare with it. (iv) Before applying the above control strategy to the actual industrial system, investigation and analysis about the optimal setting of the approximation function's order is carried out. (v) Application effects of the proposed control strategy to some industrial processes, such as copper removal process and zinc electrochemical process, are evaluated, where the system controlled output, the controller output, and the control energy are all taken into account.

The rest of this paper is organized as follows. Section II introduces the basic theories of fractional calculus and PI$^{\lambda}$D$^{\mu}$ controller in discrete domain. In section III, the proposed optimization problem and the brief description of the state transition algorithm are illustrated. In section IV, some experimental results are given to prove the effectiveness of the

TABLE 1. Conversion schemes for discretizing.

Methods	$s \to z$ conversion	Taylor series
Tustin	$s^{\alpha} \approx [\frac{2}{T}\frac{1-z^{-1}}{1+z^{-1}}]^{\alpha}$	$(\frac{2}{T})^{\alpha}[1-2\alpha z^{-1}+2\alpha^2 z^{-2}\cdots]$
Al-Alaoui	$s^{\alpha} \approx [\frac{8}{T}\frac{1-z^{-1}}{7+z^{-1}}]^{\alpha}$	$(\frac{8}{T})^{\alpha}[\frac{1}{7^{\alpha}}-\frac{8\alpha}{7^{\alpha+1}}z^{-1}+\frac{8\alpha(4\alpha-3)}{7^{\alpha+2}}z^{-2}\cdots]$
backward Euler/Grünwald-Letnikov	$s^{\alpha} \approx [\frac{1}{T}(1-z^{-1})]^{\alpha}$	$(\frac{1}{T})^{\alpha}[1-\alpha z^{-1}+\frac{\alpha(\alpha-1)}{2}z^{-2}\cdots]$
implicit Adams	$s^{\alpha} \approx [\frac{2}{T}\frac{1-z^{-1}}{3-z^{-1}}]^{\alpha}$	$(\frac{2}{T})^{\alpha}[\frac{1}{3^{\alpha}}-\frac{2\alpha}{3^{\alpha+1}}z^{-1}+\frac{2\alpha(\alpha-2)}{3^{\alpha+2}}z^{-2}\cdots]$

proposed strategy. Section V illustrates the main conclusions of this paper.

II. DISCRETE-TIME FRACTIONAL-ORDER CONTROL SYSTEM AND PI$^{\lambda}$D$^{\mu}$ Controller

The PI$^{\lambda}$D$^{\mu}$ controller is a general form of the classical PID controller. Therefore, some basic principles of fractional calculus will be briefly introduced before describing the FOPID controller in detail.

A. INTRODUCTION OF FRACTIONAL-ORDER CALCULUS

The fractional-order calculus, which is denoted as ${}_{t_0}\mathcal{D}_t^{\alpha}$ (where α represents the fractional order, t_0 and t are the lower and upper limits of the operation, respectively), is differential and integral general form in non-integer order operator. And it can be expressed by Eq. (1).

$$ {}_{t_0}\mathcal{D}_t^{\alpha} = \begin{cases} \dfrac{d^{\alpha}}{dt^{\alpha}} & \mathbf{R}(\alpha) > 0, \\ 1 & \mathbf{R}(\alpha) = 0, \\ \int_{t_0}^{t}(d\tau)^{-\alpha} & \mathbf{R}(\alpha) < 0, \end{cases} \tag{1} $$

where $\alpha \in \mathbb{R}$ is the real number.

Various kinds of principles are used to definite the fractional-order calculus, but the most widely used ones are Riemann-Liouville (RL) and Grunwald-Letnikov (GL).

(i) Riemann-Liouville definition (RL)

$$ {}_{t_0}\mathcal{D}_t^{\alpha} f(t) = \frac{1}{\Gamma(l-\alpha)}\frac{d^l}{dt^l}\int_{t_0}^{t}\frac{f(\tau)}{(t-\tau)^{1-(l-\alpha)}}d\tau, \tag{2} $$

where $l-1 < \alpha < l$, and $\Gamma(\cdot)$ is defined as the well-known Euler's gamma function that can be expressed by the following formula.

$$ \Gamma(z) = \int_0^{\infty} t^{z-1}e^{-t}dt, \quad \mathbf{R}(z) > 0. \tag{3} $$

(ii) Grünwald-Letnikov definition (GL)

$$ {}_{t_0}\mathcal{D}_t^{\alpha} f(t) = \lim_{h\to 0}\frac{1}{h^{\alpha}}\sum_{j=0}^{[(t-t_0)/h]}(-1)^j\binom{\alpha}{j}f(t-jh), \tag{4} $$

where $(-1)^j\binom{\alpha}{j}$ is the binomial coefficient of $(1-z)^{\alpha}$. In order to calculate the fractional calculus, a numerical computation method, which can be expressed by the following formula, is provided in this paper.

$$ {}_{t_0}\mathcal{D}_t^{\alpha} f(t) = \frac{1}{h^{\alpha}}\sum_{j=0}^{[(t-t_0)/h]}\upsilon_j^{(\alpha)}f(t-jh), \tag{5} $$

here,

$$ \upsilon_0^{(\alpha)} = 1, \ \upsilon_j^{(\alpha)} = (1-\frac{\alpha+1}{j})\upsilon_{j-1}^{(\alpha)}, \quad j = 1, 2, \cdots. \tag{6} $$

The Laplace transformation of fractional differential and integral of $f(t)$ can be expressed by the following formula

$$ \begin{aligned} \mathscr{L}\{\mathcal{D}^{-\alpha}f(t)\} &= s^{-\alpha}F(s), \\ \mathscr{L}\{\mathcal{D}^{\alpha}f(t)\} &= s^{\alpha}F(s) - \sum_{\kappa=0}^{l-1}s^{\kappa}[\mathcal{D}^{\alpha-\kappa-1}f(t)]_{t=0}, \\ & \qquad l-1 < \alpha < l. \end{aligned} \tag{7} $$

Due to $\binom{\alpha}{j} = \frac{\Gamma(\alpha+1)}{j!\Gamma(\alpha-j+1)}$, the RL definition is the same as the GL definition. However, in this paper we use the GL definition because it is more suitable for numerical calculations.

B. DISCRETE-TIME APPROXIMATION OF FRACTIONAL CALCULUS

In general, we can use the generating function $s \approx \psi(z^{-1})$ to represent the discretization of continuous fractional integral and differential term $s^{\mp\alpha}$, where $\psi(z^{-1})$ is a function of the complex variable z or the shift operator z^{-1} named discrete operator. Meanwhile, $\psi(z^{-1})$ and its extended form determine the effect of the approximation process.

Then we analyze several discrete-time approximations to fractional derivatives and integrals, and in general, the generating function $\psi(z^{-1})$ can be expressed by the following formula [30]

$$ \psi(z^{-1})^{\mp\alpha} = (\frac{1}{\beta T}\frac{1-z^{-1}}{\gamma+(1-\gamma)z^{-1}})^{\mp\alpha} \tag{8} $$

where T is described as the sampling period, β is the gain tuning parameter, and γ is denoted as the phase tuning parameter. For instance, when $\beta = 1$ and $\gamma = \{1/2, 7/8, 1, 3/2\}$, the generating function (8) becomes the Tustin, the Al-Alaoui, the backward Euler and the implicit Adams rules, respectively. And these conversion methods are represented in Table 1. In this paper, the Tustin rule is applied, since it is more accurate compared to other rules [1],

which leads to the generating function $\psi(z^{-1})$ becomes the following general form:

$$s^{\alpha} = \psi(z^{-1})^{\alpha} = (\frac{2}{T}\frac{1-z^{-1}}{1+z^{-1}})^{\alpha} \tag{9}$$

As it is shown in Table 1, the function of z generated by the fractional transformation is non-rational. Therefore, we expand it based on the Taylor series to obtain a rational expression, and then study n-term truncated series so that the generating formula can be adjusted more precisely. Moreover, the expression of the rational function of Eq. (9) is as follows:

$$s^{\alpha} = \psi(z^{-1})^{\alpha} = (\frac{2}{T})^{\alpha}\sum_{n=0}^{\infty} f_n(\alpha)z^{-n} \tag{10}$$

where $f_n(\alpha)$ is the coefficient which can be calculated by Eq. (11)

$$f_n(\alpha) = \frac{1}{n!}\frac{d^n}{d(z^{-1})^n}(\frac{1-z^{-1}}{1+z^{-1}})^{\alpha}\Big|_{z^{-1}=0} \tag{11}$$

Obviously, the upper bound of summation in Eq. (10) cannot be equal to infinity in practice. In this paper, we restrict the upper bound of the formula to N, the following formula is proposed:

$$s^{\alpha} = \psi(z^{-1})^{\alpha} = (\frac{2}{T})^{\alpha}\sum_{n=0}^{N} f_n(\alpha)z^{-n} \tag{12}$$

Now we summarize the first 9 coefficients of Eq. (12) in Table 2.

TABLE 2. Table of formulas $f_n(\alpha)$ for n = 0,...,8.

n	$f_n(\alpha)$
0	1
1	-2α
2	$2\alpha^2$
3	$-\frac{2}{3}\alpha - \frac{4}{3}\alpha^3$
4	$\frac{4}{3}\alpha^2 + \frac{2}{3}\alpha^4$
5	$-\frac{2}{5}\alpha - \frac{4}{3}\alpha^3 - \frac{4}{15}\alpha^5$
6	$\frac{46}{45}\alpha^2 + \frac{8}{9}\alpha^4 + \frac{4}{45}\alpha^6$
7	$-\frac{2}{7}\alpha - \frac{56}{45}\alpha^3 - \frac{4}{9}\alpha^5 - \frac{8}{315}\alpha^7$
8	$\frac{88}{105}\alpha^2 + \frac{44}{45}\alpha^4 + \frac{8}{45}\alpha^6 + \frac{2}{315}\alpha^8$

C. THE FORM OF DISCRETE-TIME PI$^{\lambda}$D$^{\mu}$ CONTROLLER

The transfer function of PI$^{\lambda}$D$^{\mu}$ in the Laplace transform domain, which was first proposed by Podlubny [2], has the following form

$$G_c(s) = \frac{U(s)}{E(s)} = k_p + k_i s^{-\lambda} + k_d s^{\mu} \tag{13}$$

where k_p, k_i and k_d are the proportional, integral and differential gains, respectively; λ and μ are integral and differential orders correspondingly.

Note that Eq. (12) holds for both the positive and negative values of α. Hence, one may try to expand the integral term of Eq. (13) in a similar manner and arrive at an equation like Eq. (12), but the problem with such an expansion is that the resulted series does not have infinite direct current gain (considering the fact that any infinite series must be truncated in practice), which is essential for tracking the step command without steady-state error [1]. In order to find a series approximation for $s^{-\lambda}$ in terms of z^{-1} which has infinite direct current gain, first we write it as $s^{-\lambda} = (1/s) \times s^{1-\lambda}$ and then apply the Tustin method to it. Finally we get the following expression:

$$s^{-\lambda} = (\frac{2}{T})^{-\lambda}\frac{1+z^{-1}}{1-z^{-1}}\sum_{n=0}^{N} f_n(1-\lambda)z^{-n} \tag{14}$$

where $f_n(1-\lambda)z^{-n}$ are again calculated from Eq. (11).

Substitution of Eq. (12) and Eq. (14) in Eq. (13) results in the following formulation for the discrete-time PI$^{\lambda}$D$^{\mu}$ controller

$$G_c(z) = K_p + K_i\frac{1+z^{-1}}{1-z^{-1}}\sum_{n=0}^{N} f_n(1-\lambda)z^{-n} + K_d\sum_{n=0}^{N} f_n(\mu)z^{-n} \tag{15}$$

where

$$K_p = k_p,\ K_i = k_i(\frac{2}{T})^{-\lambda},\quad K_d = k_d(\frac{2}{T})^{\mu} \tag{16}$$

By using the inverse z-transform, the difference equation relating $e(k)$ to $u(k)$ can be written as the following:

$$\begin{aligned} u(k) = {} & u(k-1) + K_p[e(k) - e(k-1)] \\ & + K_i\sum_{n=0}^{N} f_n(1-\lambda)[e(k-n)+e(k-n-1)] \\ & + K_d\sum_{n=0}^{N} f_n(\mu)[e(k-n) - e(k-n-1)] \end{aligned} \tag{17}$$

where the upper bound N of summation in Eq. (17) should approach ∞ ideally, but in practice it can't be considered equal to infinity. Hence, we will study the effect of parameter N on system response performance in this paper. Based on this design idea, we will further apply this controller to the loops of complex industrial processes. And the digital controllers will be implemented since most industrial plants use DCS or PLC control systems, the processor will continuously execute the incremental DFOPID algorithm. In addition, the parameters can be changed by modifying the software, which is more flexible.

III. CONTROLLER PARAMETERS OPTIMIZATION BASED ON STATE TRANSITION ALGORITHM

A. OPTIMIZATION PROBLEM FORMULATION

Fig.1 shows a block diagram of a closed-loop control system with a DFOPID controller, where $y(k)$ is regarded as the actual output of the system at the sampling point and $y_r(k)$ is the system's reference output.

In this study, the optimization algorithm will be applied to select the optimal parameters of DFOPID controller, including N, K_p, K_i, K_d, λ, and μ. In the previous study, we found

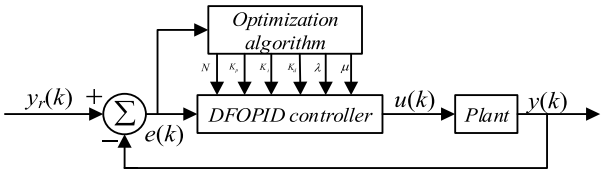

FIGURE 1. The closed-loop control system with discrete-time PI$^{\lambda}$D$^{\mu}$ controller.

that the integral time absolute error (ITAE) has excellent capability of tracking performance, strong robustness and anti-disturbance [29]. Hence, the objective function based on ITAE is defined in the following:

$$\min H(K_{p,j}, K_{i,j}, K_{d,j}, \lambda_j, \mu_j) = \sum_{j=1}^{J}\sum_{k=1}^{M} \omega_j k|e_j(k)|$$

$$s.t. \begin{cases} u_j(k) = g_j(u_j(k-1), e_j(k-n), k, \theta_j) \\ u_j^{min} \le u_j(k) \le u_j^{max} \\ \sum_{j=1}^{J} \omega_j = 1 \\ k \in [0, M] \end{cases} \tag{18}$$

where, M is the sample size, J is the total number of closed-loop control systems, $e_j(k)$ denotes error signal of the jth closed-loop control system which is determined by $e_j(k) = y_{r,j}(k) - y_j(k)$, $\theta_j = [K_{p,j}, K_{i,j}, K_{d,j}, \lambda_j, \mu_j]$ are the controller parameters of the jth control system, and ω_j represent the weighting coefficients of which values are calculated on the basis of the industrial data.

In the following parts, a novel intelligent optimization search algorithm called state transition algorithm will be adopted to solve optimization problem of discrete-time PI$^{\lambda}$D$^{\mu}$ controller design. Next, the brief description of this intelligent optimization method will be provided.

B. THE BRIEF DESCRIPTION OF STATE TRANSITION ALGORITHM

State transition algorithm(STA) is a kind of intelligent optimization search algorithm based on state transition and state space. In STA, a solution to an optimization problem and the process of updating the current solution can be considered as a state and a state transition, respectively. Generally speaking, the unified form of candidate solutions generated by STA can be expressed by the following formula:

$$\begin{cases} \boldsymbol{x}_{k+1} = A_k \boldsymbol{x}_k + B_k \boldsymbol{u}_k \\ y_{k+1} = f(\boldsymbol{x}_{k+1}) \end{cases}, \tag{19}$$

where $\boldsymbol{x}_k \in \mathbb{R}^n$ is defined as a state that corresponds to the current solution to an optimization problem; $\boldsymbol{u}_k$ is defined as a function of $\boldsymbol{x}_k$; A_k and B_k are the state transition coefficient matrices with proper dimensions, respectively; f is treated as the evaluation or objective function.

There are four special state transformation operators to generate candidate solutions.

(a) Rotation transformation

$$\boldsymbol{x}_{k+1} = \boldsymbol{x}_k + \varepsilon_r \frac{1}{n\|\boldsymbol{x}_k\|_2} R_r \boldsymbol{x}_k, \tag{20}$$

where the rotation transformation can search on a hypersphere with a given radius ε_r, which is a local search operator. $R_r \in \mathbb{R}^{n\times n}$ is a random matrix of which elements are in the range of [-1, 1]; $\|\cdot\|_2$ is the 2-norm of a vector; ε_r is a positive constant term called the rotation factor.

(b) Translation transformation

$$\boldsymbol{x}_{k+1} = \boldsymbol{x}_k + \varepsilon_t R_t \frac{\boldsymbol{x}_k - \boldsymbol{x}_{k-1}}{\|\boldsymbol{x}_k - \boldsymbol{x}_{k-1}\|_2}, \tag{21}$$

where the translation transformation has a function of searching on a line. $R_t \in \mathbb{R}$ is a random variable of which elements are in the range of [0,1]; ε_t is regarded as a positive constant term called the translation factor.

(c) Expansion transformation

$$\boldsymbol{x}_{k+1} = \boldsymbol{x}_k + \varepsilon_e R_e \boldsymbol{x}_k, \tag{22}$$

where the expansion transformation, which is defined as a global search operator, can search in the whole space. $R_e \in \mathbb{R}^{n\times n}$ is a random diagonal matrix, and its elements obey the Gaussian distribution of which mean value is 0 and standard deviation is 1; ε_e is described as a positive constant term called the expansion factor.

(d) Axesion transformation

$$\boldsymbol{x}_{k+1} = \boldsymbol{x}_k + \varepsilon_a R_a \boldsymbol{x}_k \tag{23}$$

where the axesion transformation, which is defined as a global search operator, can strengthen the single dimensional. $R_a \in \mathbb{R}^{n\times n}$ is a random diagonal matrix, and its elements obey the Gaussian distribution of which mean value is 0 and standard deviation is 1; ε_a is regarded as a positive constant term called the axesion factor.

The procedure of the basic STA are shown in the Algorithm 1. The flowchart of state transition algorithm

In STA, the "greedy criterion" is adopted to update the new best solution. SE is the degree of search enforcement which represents the times of transformation by a certain operator. *funfcn* is the objective function, *GBest* represents candidate solution set, *Best* is the current best solution. $\varepsilon_{r\,\max}$ and $\varepsilon_{r\,\min}$ are the maximum value and maximum value of the rotation factor, respectively. The rotation factor is reducing from the $\varepsilon_{r\,\max}$ to the $\varepsilon_{r\,\min}$ in the way of exponential function of which base is fc (lessening coefficient). Meanwhile, the specified termination criterion in this paper is the maximum number of iterations reaches to *Maxiter*.

In terms of the computational complexity, for a n dimensional optimization problem, the computational complexity of the expansion transformation operator, rotation transformation operator and axesion transformation operator is $O(n * SE)$ in each iteration. The translation transformation is only used when certain conditions are met. If used, the computational complexity is also $O(n * SE)$. Moreover, the calculation of objective function requires $O(n * SE)$ computations.

Algorithm 1 Pseudocode of the Continuous STA

Step 1: Set the maximum number of interations *Maxiter*, the search enforcement *SE*, and the initial solution *Best*.
Step 2: While the specified termination criterion isn't satisfied
DO
FOR i=1 to *maxiter*
Step 2.1: if $\varepsilon_r < \varepsilon_{r\min}$ then
$\varepsilon_r \leftarrow \varepsilon_{r\max}$
end if
Step 2.2: expansion step
GBest ← expansion(funfcn,Best,SE,ε_e)
if fGBest < fBest then
fBest ← fGBest & Best ← GBest
GBest ← translation(funfcn,Best,SE,ε_t)
if fGBest < fBest then
fBest ← fGBest & Best ← GBest
end if
end if
Step 2.3: rotation step
GBest ← rotation(funfcn,Best,SE,ε_r)
if fGBest < fBest then
fBest ← fGBest & Best ← GBest
GBest ← translation(funfcn,Best,SE,ε_t)
if fGBest < fBest then
fBest ← fGBest & Best ← GBest
end if
end if
Step 2.4: axesion step
GBest ← axesion(funfcn,Best,SE,ε_a)
if fGBest < fBest then
fBest ← fGBest & Best ← GBest
GBest ← translation(funfcn,Best,SE,ε_t)
if fGBest < fBest then
fBest ← fGBest & Best ← GBest
end if
end if
Step 2.5: $\varepsilon_r \leftarrow \frac{\varepsilon_r}{fc}$
Step 3: $Best^* \leftarrow Best$

Therefore, taking into account all the above computations and the iterations, the overall computational complexity of the STA is $O(n * SE * Maxiter)$.

C. DIAGRAM OF CONTROL STRATEGY BASED ON DFOPID

The diagram of the control strategy based on DFOPID is shown in Fig.2.

Based on the Tustin operator and its Taylor series, the novel DFOPID control strategy is proposed. In addition, the control systems are also discretized through this discretization method. Then, the optimization model based on the ITAE is proposed and state transition algorithm is investigated for solving the aforementioned optimization problem. However, before applying the state transition algorithm to this optimization problem, it is necessary to compare and select the upper bound N of the DFOPID controller. By using this optimization method, we obtain the optimization parameters of DFOPID and PID. Then different optimization algorithms are applied to adjust the DFOPID controller. In order to prove the superiority of DFOPID control strategy and the competitiveness of STA in solving such optimization problems, the system response performance, control energy, variation of control signals, the results of rank sum test of the objective function values obtained by multiple experiments, as well as the convergence rate of different algorithms are analyzed.

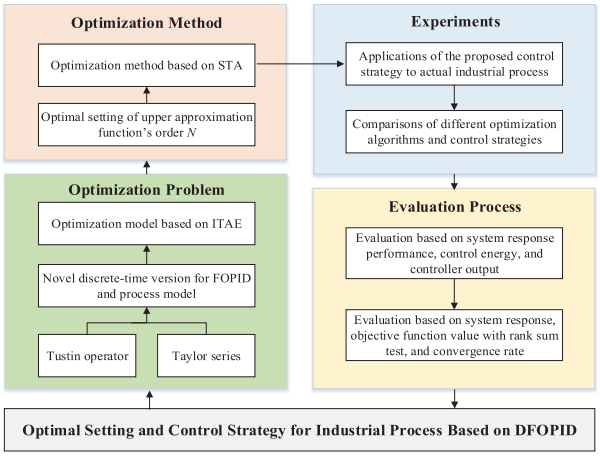

FIGURE 2. The diagram of control strategy for industrial process based on the DFOPID.

IV. EXPERIMENTAL RESULTS AND DISSCUSSION

In the procedure of designing the DFOPID controller, the optimization algorithms are adopted to minimize the integral time absolute error (ITAE). In this paper, STA is used to adjust the parameters of controllers. Meanwhile, the parameter settings of the algorithm are the same as previous study [18], which are provided as follows: $fc = 2$, $SE = 30$, $Maxiter = 100$, $\varepsilon_{r\max} = 1$, $\varepsilon_{r\min} = 1e-4$, $\varepsilon_t = 1$, $\varepsilon_e = 1$, $\varepsilon_a = 1$. These optimal values are experimentally determined under conducting a series of additional experiments with different parameters.

A. CONTROLLER VERIFICATION AND PARAMETER SETTING

In the first place, we change the value of N to study the influence of this precondition on system response performance. In addition, another three optimization algorithms namely comprehensive learning particle swarm optimization (CLPSO) algorithm [31], genetic algorithm (MATLAB genetic algorithm toolbox v1.2), and violation learning differential evolution (VLDE) algorithm [32] are adopted to compare with STA. In order to reflect the fairness of comparison, the population size or degree of search enforcement (SE = 30) and the maximum iterations (Maxiter = 100) are the same. In addition, the design of the CLPSO algorithm

TABLE 3. Controller gains for DFOPID and PID of the example.

Controllers	K_p	K_i	K_d	λ	μ
DFOPID(N=2)	1.3734	0.0106	0.0124	0.5667	3.5130
DFOPID(N=5)	1.2629	0.0787	5.1220	0.0107	0.3875
DFOPID(N=8)	1.0708	0.0752	3.6076	0.0214	0.3459
PID	2.8031	0.0353	5.7135	-	-

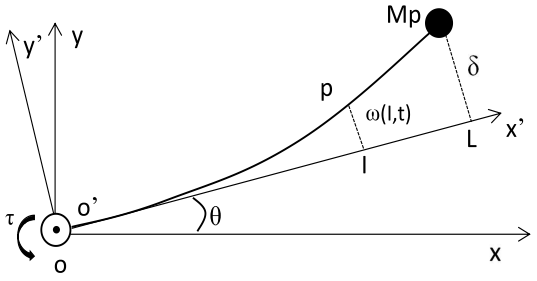

FIGURE 3. The schematic of the one-link flexible robot arm.

is described in detail in [31]. And in this paper, the learning probability P_l for each particle is set by $P_{li} = 0.05 + 0.45 * \frac{exp(\frac{10(i-1)}{ps})-1}{exp(10)-1}$, where ps is the population size, i represents the ith population. Furthermore, the refreshing gap parameter m is zero. For the genetic algorithm, there are three arithmetic operators including the select operator (Stochastic Universal Sampling, it performs selection with stochastic universal sampling), the crossover operator (Crossover Single-Point, it can perform single-point crossover between paired individuals and return the current generation after mating, and the crossover probability P_c is 0.7) and the mutuation operator (This operator represents the current population which can mutate each element with given probability and return the resulting population, and the mutation probability P_m is 0.05). Furthermore, more information about the VLDE algorithm can be found in [32].

Next, the following example is investigated in this study.

Applying the discrete-time PI$^{\lambda}$D$^{\mu}$ to the system of one-link flexible robot arm [33]. And Fig.3 shows schematic of it, which rotates horizontally, with the transfer function appears as

$$G(s) = \frac{-4.906s^2 - 0.5884s + 335.17}{s^4 + 0.55437s^3 + 139.6s^2 + 27.91s}. \quad (24)$$

Then the discrete dynamic equation of above system (24) can be described as follows based on the Tustin rule and sampling time $T = 0.1$:

$$\begin{aligned} y(k+1) &= 2.933y(k) - 3.841y(k-1) + 2.863y(k-2) \\ &-0.9548y(k-3) - 0.007422u(k+1) + 0.005964u(k) \\ &+0.02688u(k-1) + 0.006178u(k-2) - 0.007315u(k-3) \end{aligned} \quad (25)$$

Fig.4 shows the nyquist diagram, root locus, bode diagram and pole-zero map of the example. This system, apparently, is a non-minimum phase process with oscillatory poles and the step response steady state error cannot be eliminated without controller. Therefore, the DFOPID controller is applied to this system.

The solution space of Eq. (17) is five dimensional-$\{\lambda, \mu, K_p, K_i, K_d\}$. To reduce the time of optimal process, the initial range of the controller parameters for this example are limited in $\lambda \in [0, 5]$, $\mu \in [0, 5]$, $K_p \in [0, 10]$, $K_i \in [0, 10]$, and $K_d \in [0, 10]$. But before determining the five parameters of controller, we should choose a suitable value of N in Eq. (17). Hence, simulation is carried out under the different values of N. The optimal controller gains for DFOPID and PID are provided in Table 3.

The unit step response and the controller output based on different values of N are given in Figs. 5, 6 and 8. It is shown that the larger the value is, the better system's response performance and the smaller variation of the controller output signal will be. Then, we also perform an analysis on the control energy(CE) which is obtained by Eq. (26).

$$CE = \sum_{k=1}^{M} |u(k)| \quad (26)$$

Table 4 shows that the DFOPID controller with $N = 8$ has the lowest control energy. Nevertheless, the time of parameters optimization will increase when the value increases since the calculation of $u(k)$ from Eq. (17) totally needs $2N + 3$ multiplications and $2N + 6$ summations at each sampling period. Hence, this paper uses $N = 8$ after taking into account the response performance and the practical efficiency.

TABLE 4. The control energy for different controllers.

	DFOPID(N=2)	DFOPID(N=5)	DFOPID(N=8)	PID
CE	16.4715	13.1725	9.5025	14.6072

Moreover, we also obtained the system controlled output and the PID controller output. As it can be observed in Figs. 7 and 8, the DFOPID controller results in a more satisfactory response performance controller output when compared with conventional PID controller.

In the following, 30 independent simulations are performed for each algorithm. And all of these algorithms are carried out under the MATLAB(Version R2015b). The best, mean, and worst objective function values as well as the standard deviation are calculated after 30 simulations to evaluate the performance of these algorithms.

The experimental procedure and parameters setting are same with the previous example. The best parameters, which

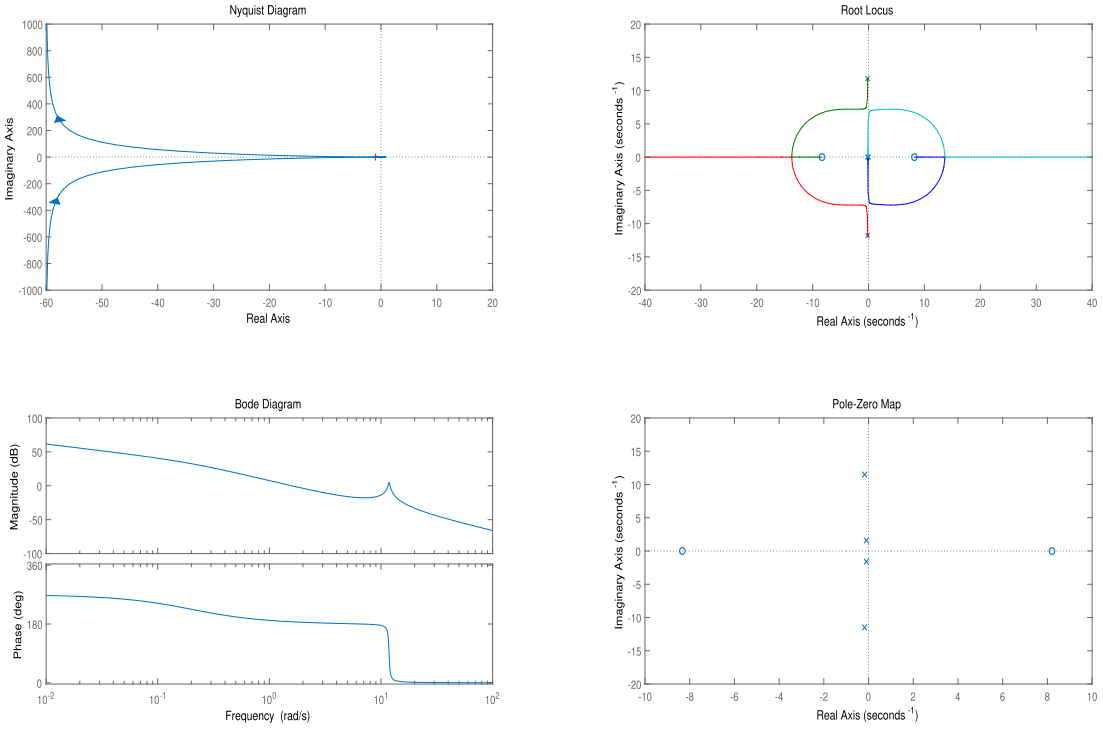

FIGURE 4. The nyquist diagram, root locus, bode diagram and pole-zero map.

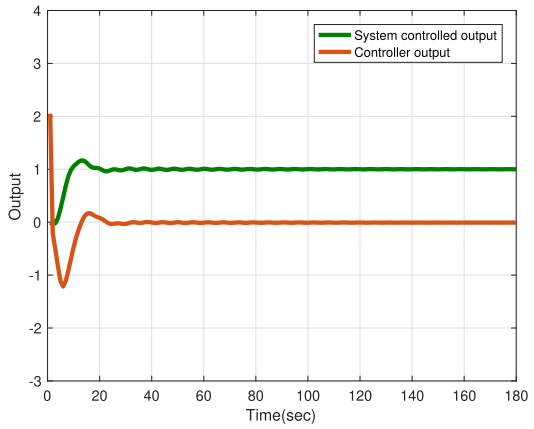

FIGURE 5. Unit step response with N=2.

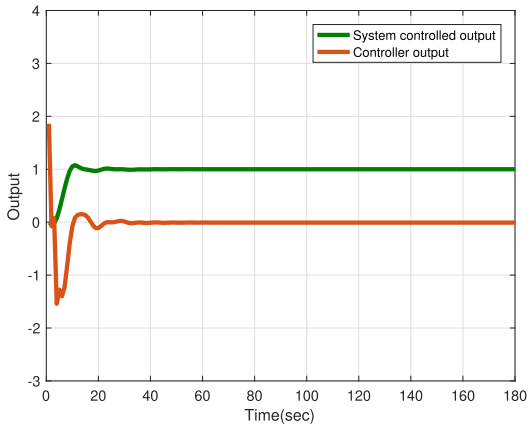

FIGURE 6. Unit step response with N=5.

are found by STA, GA, CLPSO, and VLDE, are given in the Table 5. In addition, the detailed statistical results obtained by different algorithms are shown in Table 6. From Table 6, it can be seen that STA can find the minimum value with a high probability, indicating that STA is more suitable for this optimization problem. In addition, the Wilcoxon rank sum test [34] is applied to analyze the performance of these three different optimization algorithms, and the results in Table 7 demonstrate that there is a significant difference between the STA and the other two algorithms. Again, Fig.9 and Fig.10 show that STA can find the optimal parameters which lead the system into stable in a much faster way, since the trajectories of the objective function value show that STA can converge to the global optimal solution at 25 iterations.

B. INDUSTRIAL EXPERIMENTS

1) COPPER REMOVAL PROCESS

The proposed control strategy is applied to the copper removal process in a zinc hydrometallurgy of China. As shown in Fig. 11, the zinc sulfate solution to be purified flows into several connected continuous stirred reactors, and then the copper ions in the solution are gradually removed by adding zinc powder to each reactor. Next, the solution will be solid-liquid separated in a thickener. In the copper removal process, the copper ion concentration in the solution

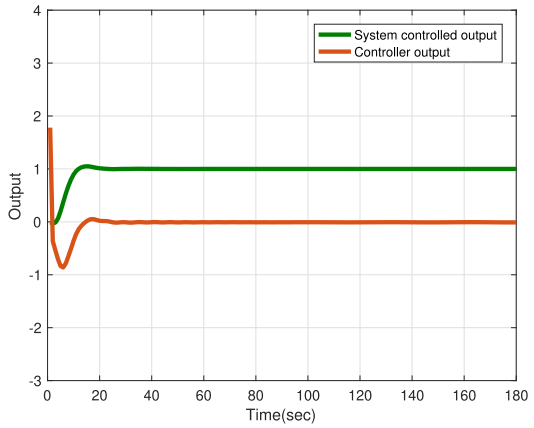

FIGURE 7. Unit step response with N=8.

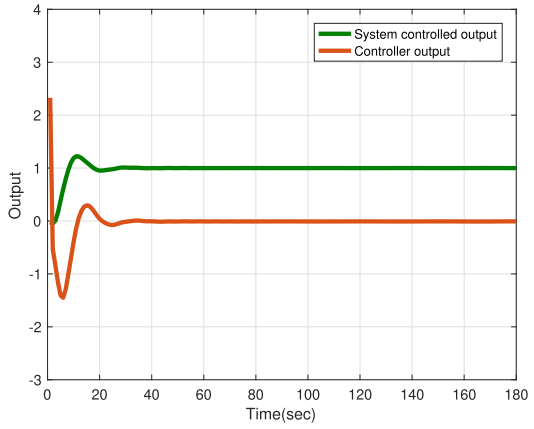

FIGURE 8. Unit step response with integer order PID controller.

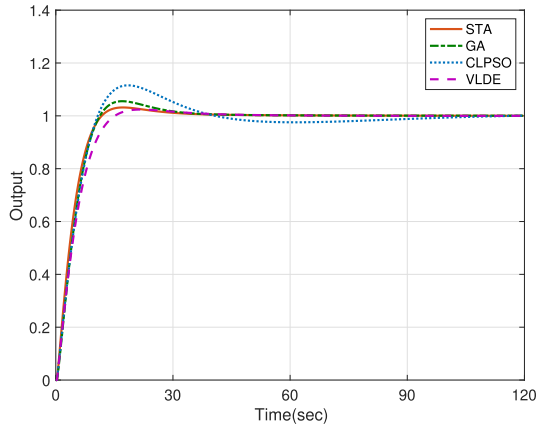

FIGURE 9. Unit step response of the closed-loop system.

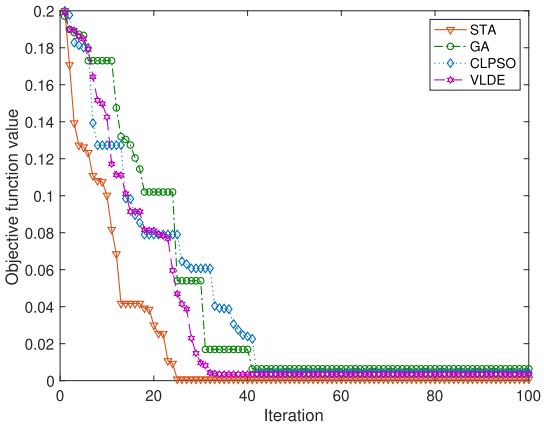

FIGURE 10. Iterative curves of the objective function values obtained by different methods.

is determined by the amount of zinc powder added. Higher copper ion concentration will reduce the current efficiency of the zinc electrolysis process and the quality of the zinc ingot. However, an appropriate copper ion in the solution can increase the removal efficiency of the next cobalt removal process. Therefore, the copper ion concentration should be strictly controlled within the required range. Due to the nonlinearity and coupling factors existing in the copper removal process, it is difficult to ensure the copper ion concentration at the outlet is stable.

In this paper, we take the copper removal process in the Zhuzhou smeltery of Hunan province as an example to study the proposed control strategy. The copper removal process of this plant consists of two continuous stirred reactors and one thickener. According to the principle of mass balance, the copper removal process model can be expressed by the following equations [35]:

$$\begin{aligned} V\dot{C}_{Cu^{2+},1}(t) &= QC^0_{Cu^{2+},1}(t) - (1+q)\,QC_{Cu^{2+},1}(t) \\ &\quad -(a_1u_{Zn,1}(t)+a_2)C_{Cu^{2+},1}(t) \\ V\dot{C}_{Cu^{2+},2}(t) &= (1+q)\,QC^0_{Cu^{2+},2}(t) - (1+q)\,QC_{Cu^{2+},1}(t) \\ &\quad -(a_3u_{Zn,2}(t)+a_4)C_{Cu^{2+},2}(t) \end{aligned} \tag{27}$$

where V is the volume of the reaction solution, $C^0_{Cu^{2+},j}, j = 1, 2$ are the copper ion concentration, $\dot{C}_{Cu^{2+},j}, j = 1, 2$ represent the changing rate of copper ion concentration, $C^0_{Cu^{2+},j}, j = 1, 2$ denote the copper ion concentration at the inlet, $u_{Zn,j}, j = 1, 2$ are the addition rate of zinc powder, Q indicates the flow rate of the solution, and q is the returned underflow's flow rate. a_1, a_2, a_3, and a_4 are the parameters determined by the industrial data. Here, $a_1 = 0.0208$, $a_2 = 0.1387$, $a_3 = 0.0003$, and $a_4 = 0.9410$. In addition, we assume $C^0_{Cu^{2+},2}(t) = C_{Cu^{2+},1}(t_{end})$ since the reactors are connected.

On the basis of the forward-Euler difference principle, the discrete-time model of the copper removal process is transformed into the following version:

$$\begin{aligned} C_{Cu^{2+},1}(k+1) &= hQV^{-1}C^0_{Cu^{2+},1}(k) \\ &\quad -(h\,(1+q)\,QV^{-1}-1)C_{Cu^{2+},1}(k) \\ &\quad -h(a_1u_{Zn,1}(k)+a_2)V^{-1}C_{Cu^{2+},1}(k) \\ &:= g_1(C_{Cu^{2+},1}(k), u_{Zn,1}(k), k) \\ C_{Cu^{2+},2}(k+1) &= h\,(1+q)\,QV^{-1}C^0_{Cu^{2+},2}(k) \\ &\quad -(h\,(1+q)\,QV^{-1}-1)C_{Cu^{2+},1}(k) \\ &\quad -h(a_3u_{Zn,2}(k)+a_4)V^{-1}C_{Cu^{2+},2}(k) \\ &:= g_2(C_{Cu^{2+},2}(k), u_{Zn,2}(k), k) \end{aligned} \tag{28}$$

where h denotes the step length.

TABLE 5. Best parameters of DFOPID with different algorithms.

algorithms	K_p	K_i	K_d	λ	μ
STA	1.0708	0.0752	3.6076	0.0214	0.3459
GA	0.3448	0.6782	7.7327	0.5007	0.3744
CLPSO	1.2738	0.0790	5.3269	0.0107	0.3923
VLDE	1.1093	0.0779	5.2929	0.9943	0.8657

TABLE 6. Objective function values under different algorithms.

algorithms	best value	mean value	st.dev	worst value
STA	8.017E-4	8.306E-4	3.835E-5	8.643E-4
GA	6.416E-3	6.684E-3	4.339E-4	6.735E-3
CLPSO	4.335E-3	4.623E-3	6.403E-4	5.201E-3
VLDE	3.521E-3	3.791E-3	4.148E-4	4.315E-3

TABLE 7. Wilcoxon rank sum test at a 0.05 significance level.

Process	STA	GA	PSO	VLDE
Flexible robot arm	8.306E-4±3.835E-5	6.684E-3±4.339E-4 −	4.623E-3±6.403E-4 −	3.791E-3±4.148E-4 −

"−","+",and "≈" denote that the steady-state error of the corresponding algorithm is worse than, better than, and similar to that of STA, respectively.

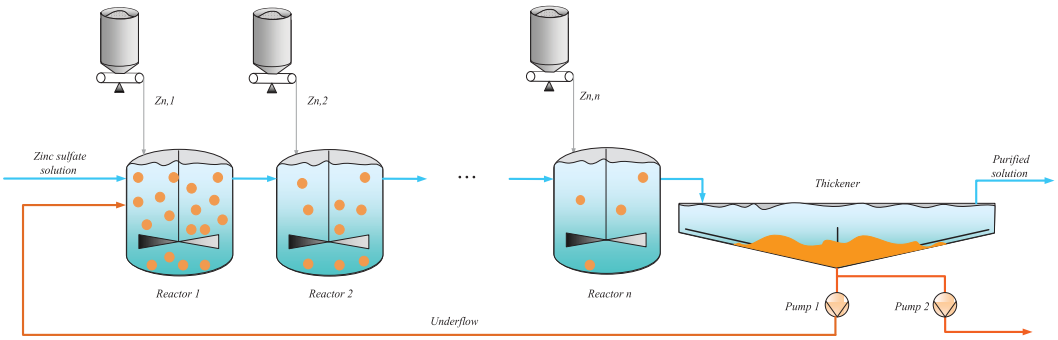

FIGURE 11. Flow diagram of the copper removal process.

Next, DFOPID is applied to the above process for making the copper ion concentration meet the process requirement. The DFOPID control strategy for this problem is described as:

$$\begin{aligned} u_{Zn,j}(k) = {} & u_{Zn,j}(k-1) + K_{p,j}[e_{Cu^{2+},j}(k) - e_{Cu^{2+},j}(k-1)] \\ & + K_{i,j}\sum_{n=0}^{8} f_n(1-\lambda)[e_{Cu^{2+},j}(k-n) \\ & + e_{Cu^{2+}j}(k-n-1)] + K_{d,j}\sum_{n=0}^{8} f_n(\mu)[e_{Cu^{2+},j}(k-n) \\ & - e_{Cu^{2+},j}(k-n-1)] \\ := {} & g_{3,j}(u_{Zn,j}(k-1), e_{Cu^{2+},j}(k-n), k, \theta_j) \end{aligned} \tag{29}$$

$$e_{Cu^{2+},j}(k) = C_{Cu^{2+},j}(k) - C^*_{Cu^{2+},j} := g_{4,j}(C_{Cu^{2+},j}(k), k) \tag{30}$$

where θ_j are the parameters to be optimized of the jth controller, $C^*_{Cu^{2+},j}$ represents the process requirement of the copper ion concentration in the jth reactor. Based on the Eq.(18), the optimal DFOPID controller parameters can be obtained by solving the following optimization problem:

$$\min\ H = \sum_{j=1}^{2}\sum_{k=0}^{M} \omega_j k |e_{Cu^{2+},j}(k)|$$

$$s.t.\ \begin{cases} C_{Cu^{2+},1}(k+1) = g_1(C_{Cu^{2+},1}(k), \quad u_{Zn,1}(k), k) \\ C_{Cu^{2+},2}(k+1) = g_2(C_{Cu^{2+},2}(k), \quad u_{Zn,2}(k), k) \\ u_{Zn,j}(k) = g_{3,j}(u_{Zn,j}(k-1), \quad e_{Cu^{2+},j}(k-n), k, \theta_j) \\ e_{Cu^{2+},j}(k) = g_{4,j}(C_{Cu^{2+},j}(k), k) \\ C^{min}_{Cu^{2+},i} \le C_{Cu^{2+},i}(k) \le C^{max}_{Cu^{2+},i} \\ u^{min}_{Zn,i} \le u_{Zn,i}(k) \le u^{max}_{Zn,i} \\ \omega_1/\omega_2 = (C^0_{Cu^{2+},2} - C^*_{Cu^{2+},2})/(C^0_{Cu^{2+},1} - C^*_{Cu^{2+},1}) \\ \omega_1 + \omega_2 = 1 \\ k \in [0, M] \end{cases} \tag{31}$$

Meanwhile, some industrial data is selected from the copper removal process in Zhuzhou smeltery. In this practical plant, these sets of data are obtained by manual operation every 2 h. Based on the industrial data, the ranges of the constraints are listed in Table. 8. Then, STA is applied to solve the aforementioned optimization problem, and the STA will run 10 times under each group of data to increase the

TABLE 8. The ranges of the different constraints.

$Reactors$	$C^0_{Cu^{2+}}(g/L)$	$C^*_{Cu^{2+}}(g/L)$	$u_{Zn}(t/h)$	Q(m^3/h)	q(m^3/h)
$1st$	[0.8 3.0]	$0.3{\cdot}C^0_{Cu^{2+},1}$+$0.7{\cdot}C^*_{Cu^{2+},2}$	[0 10]	[140 280]	[6 18]
$2ed$	$C^*_{Cu^{2+},1}$	[0.2 0.4]	[0 3]	[140 280]	-

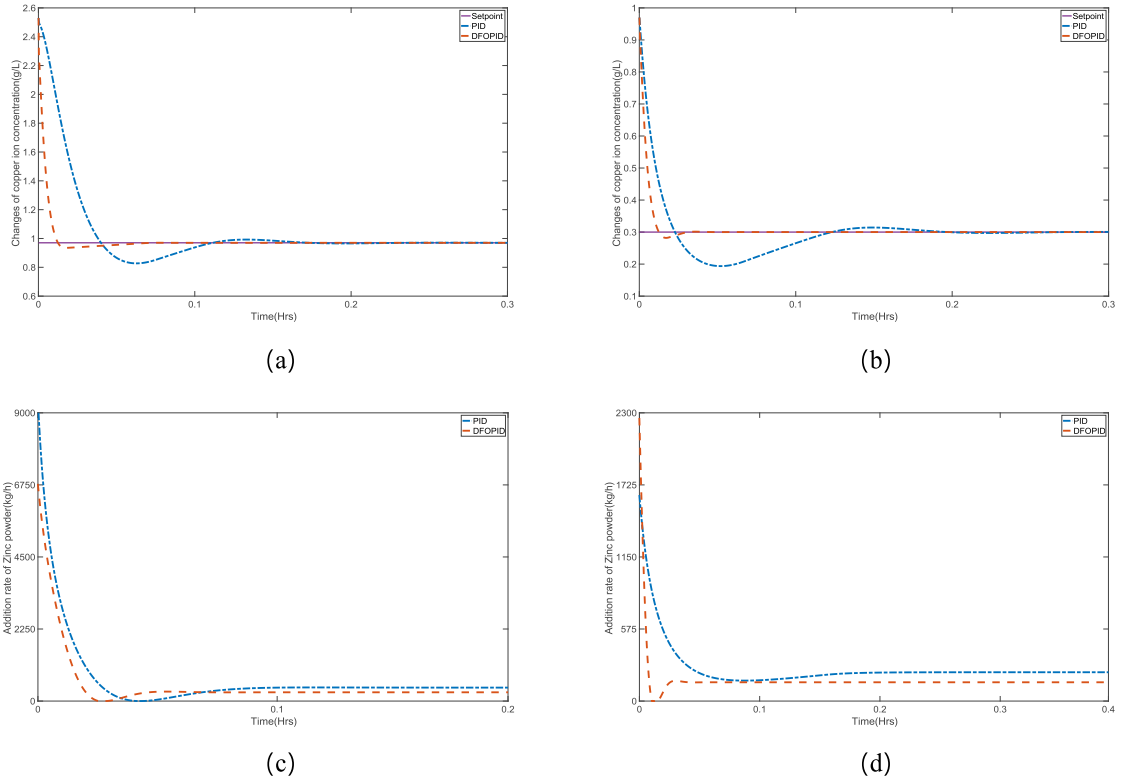

FIGURE 12. The change curves of copper ion concentration in the (a) first reactor, (b) second reactor. Addition rate of Zinc powder in the (c) first reactor, and (d) second reactor.

credibility of the optimization results. Fig. 12 shows the optimization results for one group of data under different controllers, where the copper ion concentration at inlet and the production required concentration of the two reactors are $C^0_{Cu^{2+},1} = 2.53$, $C^0_{Cu^{2+},2} = 0.97$, $C^*_{Cu^{2+},1} = 0.97$, $C^*_{Cu^{2+},2} = 0.3$, respectively. Obviously, both controllers make the copper ion concentration meet the industrial requirements, but the progress controlled by DFOPID controller has better system response performance. In addition, the control energy of DFOPID, i.e. the additive amount of zinc powder, is also less. Furthermore, the optimal parameters of the two controllers are presented in Table 9.

In the actual industrial process, the inlet-ion-concentration and the flow rate will fluctuate within small ranges during the same day. In order to further evaluate the performance of the proposed controller, tests of robustness are carried out. In this study, Gaussian noises with standard deviation of $\pm 5\%$ are applied to simulate the disturbances of inlet-ion-concentration and the flow rate. Fig. 13 shows the corresponding results of one experiment. Obviously, DFOPID controller can offer a better optimized control than PID controller in the respect of handling the fluctuation of industrial condition.

2) ELECTROCHEMICAL PROCESS OF ZINC

The electrochemical process is the last stage in zinc hydrometallurgy. As shown in Fig. 14, the recovery of zinc by electrolysis is accomplished by adding direct current (ι) to the insoluble electrodes, and the zinc sulfate solution is reduced to the metallic zinc at the cathode. The yield of zinc is directly dependent on the current applied to the electrodes. The higher the current density, the more the yield. However, the price of the electricity is adjusted continuously according to the varying load in China, which causes the cost of electricity is different at different period during the same day. Therefore, many smelters choose to increase the current density during the period of low electricity price, and run with low current density in the period of high electricity price. This not only reduces the cost of power consumption, but also helps to balance the load on the grid. Nevertheless, excessive current density in zinc electrolysis will lead to waste of the electrical energy, while too low current density can reduce current efficiency. Hence, it is necessary to control the current density stably at different pricing period to meet the production requirements of zinc output.

The seven series of electrochemical processes in the Zhuzhou smeltery are taken as the research objects. There are

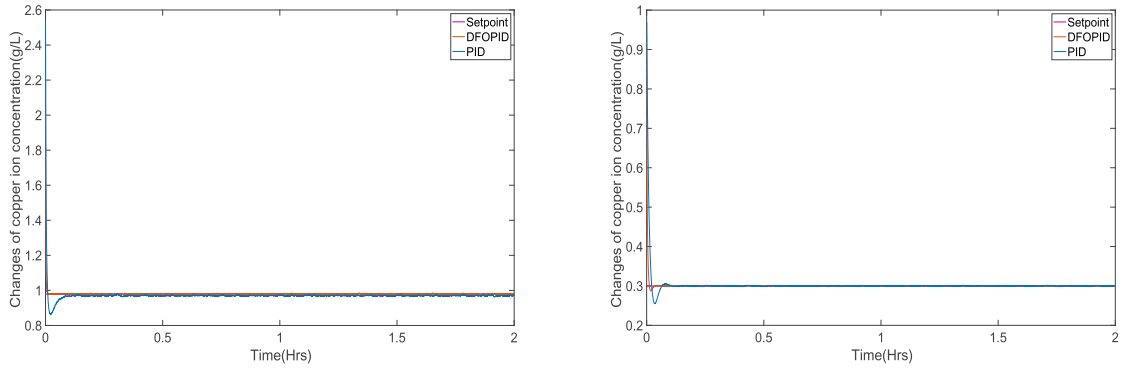

FIGURE 13. The change curves of copper ion concentration in the (a) first reactor, (b) second reactor. Addition rate of Zinc powder in the (c) first reactor, and (d) second reactor.

TABLE 9. Optimal parameters of PID and DFOPID controllers for copper removal process.

	$Reactors$	K_p	K_i	K_d	λ	μ
PID	$1st$	999.9983	6.1409	6.2016	-	-
	$2ed$	999.9998	4.6498	4.6498	-	-
DFOPID	$1st$	753.9768	0.7283	218.2465	2.0847	0.0281
	$2ed$	738.3449	12.3715	59.7542	3.4551	2.8148

four pricing periods, and the required outputs of zinc in each period are $G_{Zn,1} = 200t$, $G_{Zn,2} = 160t$, $G_{Zn,3} = 280t$, $G_{Zn,4} = 320t$, respectively. On the basis of the Faraday's laws of electrolysis, the mathematical formulation of these seven series of electrochemical processes can be described as follows [36]:

$$\begin{aligned} \dot{G}^{\eta}_{Zn,j}(t) &= \chi^{\eta} B^{\eta} S \varrho \zeta^{\eta}_{\iota,j}(t)\, u^{\eta}_{\iota,j}(t) \\ \zeta^{\eta}_{\iota,j}(t) &= \sum_{m=0}^{4} b_m \left(u^{\eta}_{\iota,j}(t)\right)^m \end{aligned} \tag{32}$$

where η and j are the counting symbols of the series of electrochemical processes and the pricing periods, respectively; $\dot{G}^{\eta}_{Zn,j}$ represent the changing rate of zinc output; χ^{η} describe the number of electrolytic cells in the ηth series; B^{η} denote the number of cathode plates in an electrolytic cell; S is the area of a plate; ϱ is the electrochemical equivalent of zinc; $u^{\eta}_{\iota,j}$ represent the current density; and $\zeta^{\eta}_{\iota,j}$ indicate the current efficiency; b_m are the coefficients need to be determined. Here, $b_0 = 0.785037$, $b_1 = 5.855\text{e}-4$, $b_2 = 2e-6$, $b_3 = 3.2094\text{e}-9$, $b_4 = -1.9052\text{e}-12$.

Similarly, the discrete-time version of the electrochemical process model and the DFOPID control strategy can be converted into as follows:

$$\begin{aligned} G^{\eta}_{Zn,j}(k+1) &= h\chi^{\eta} B^{\eta} S \varrho \zeta^{\eta}_{\iota,j}(k) u^{\eta}_{\iota,j}(k) + G^{\eta}_{Zn,j}(k) \\ &:= l_{1,j}\left(G^{\eta}_{Zn,j}(k), \zeta^{\eta}_{\iota,j}(k), u^{\eta}_{\iota,j}(k), k\right) \\ \zeta^{\eta}_{\iota,j}(k) &= \sum_{m=0}^{4} b_m \left(u^{\eta}_{\iota,j}(k)\right)^m := l_{2,j}\left(u^{\eta}_{\iota,j}(k), k\right) \\ u^{\eta}_{\iota,j}(k) &= u^{\eta}_{\iota,j}(k-1) + K_{p,j}[e^{\eta}_{Zn,j}(k) - e^{\eta}_{Zn,j}(k-1)] \\ &\quad + K_{i,j} \sum_{n=0}^{8} f_n(1-\lambda)[e^{\eta}_{Zn,j}(k-n) \\ &\quad + e^{\eta}_{Zn,j}(k-n-1)] + K_{d,j} \sum_{n=0}^{8} f_n(\mu)[e^{\eta}_{Zn,j}(k-n) \\ &\quad - e^{\eta}_{Zn,j}(k-n-1)] \\ &:= l_{3,j}(u^{\eta}_{\iota,j}(k-1), e^{\eta}_{Zn,j}(k-n), k, \theta_j) \end{aligned} \tag{33}$$

$$\begin{aligned} e^{\eta}_{Zn,j}(k) &= G^{\eta}_{Zn,j}(k) - G^{*}_{Zn,j} \\ &:= l_{4,j}(G^{\eta}_{Zn,j}(k), k) \end{aligned} \tag{34}$$

$$\tag{35}$$

where h denotes the step length; $G^{*}_{Zn,j}$ is the process requirement of the output of zinc in the jth pricing period. Meanwhile, the optimization model of this problem should be established as the following form:

$$\min\ H = \sum_{j=1}^{4} \sum_{\eta=1}^{7} \sum_{k=0}^{M} \omega^{\eta}_{j} k |e^{\eta}_{Zn,j}(k)|$$

$$\text{s.t.} \begin{cases} G^{\eta}_{Zn,j}(k+1) = !l_{1,j}\left(G^{\eta}_{Zn,j}(k), \zeta^{\eta}_{\iota,j}(k), u^{\eta}_{\iota,j}(k), k\right) \\ \zeta^{\eta}_{\iota,j}(k) = l_{2,j}\left(u^{\eta}_{\iota,j}(k), k\right) \\ u^{\eta}_{\iota,j}(k) = l_{3,j}(u^{\eta}_{\iota,j}(k-1), e^{\eta}_{Zn,j}(k-n), k, \theta_j) \\ e^{\eta}_{Zn,j}(k) = l_{4,j}(G_{Zn,j}(k), k) \\ u^{min}_{\iota,i} \le u^{\eta}_{\iota,i}(k) \le u^{max}_{\iota,i} \\ G^{*}_{Zn,j} = \begin{bmatrix} 21 & 29 & 33 & 28 & 30 & 30 & 30 \\ 17 & 23 & 26 & 22 & 24 & 24 & 24 \\ 30 & 39 & 46 & 39 & 43 & 43 & 43 \\ 32 & 44 & 52 & 44 & 48 & 48 & 48 \end{bmatrix} \\ \chi^{\eta} = [240\ 240\ 246\ 192\ 208\ 208\ 208] \\ B^{\eta} = [34\ 46\ 54\ 56\ 56\ 57\ 57] \\ S = 1.13 \\ \varrho = 1.2202 \\ \omega^{\eta}_{j} = 1/G^{*}_{Zn,j} \\ k \in [0, M] \end{cases}$$

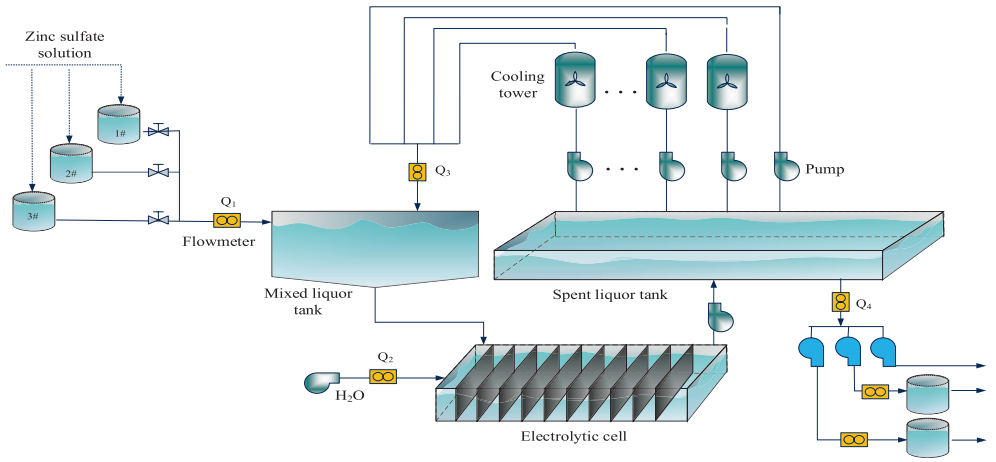

FIGURE 14. Flow diagram of the electrochemical process of zinc.

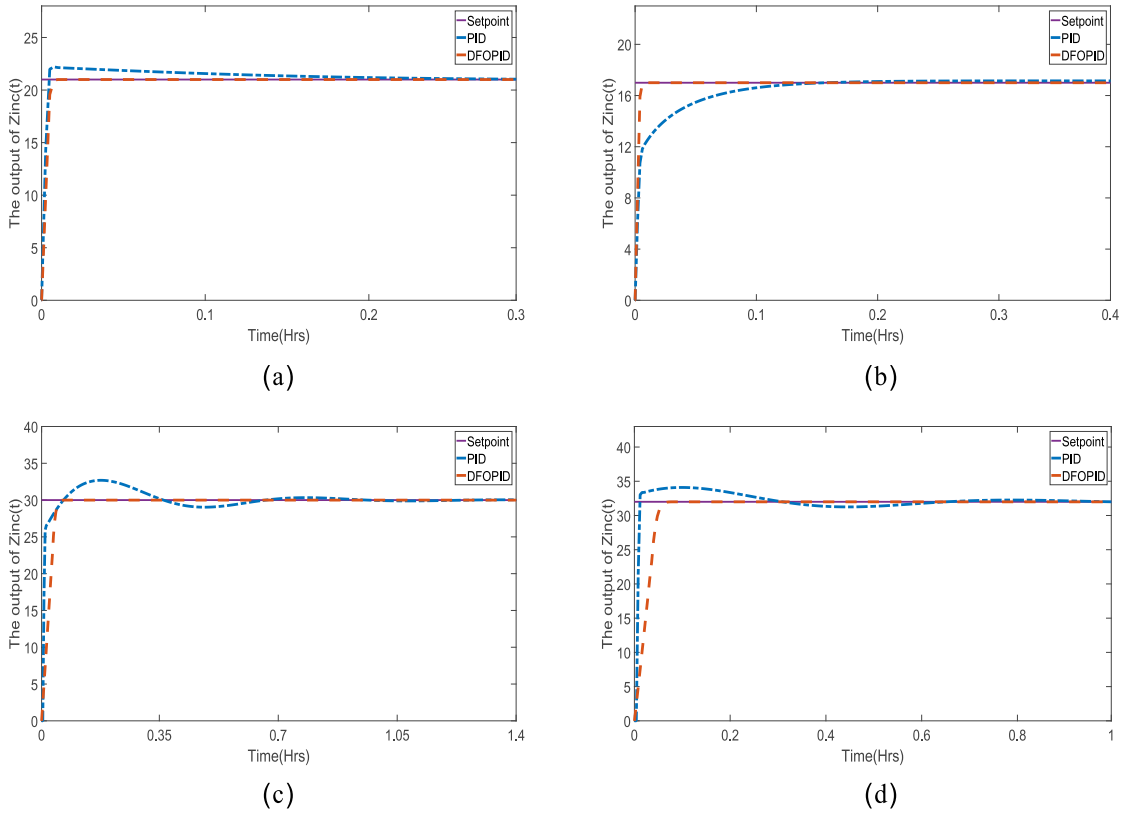

FIGURE 15. The outputs of zinc in the first series of electrochemical processes during the (a) first pricing period, (b) second pricing period, (c) third pricing period, and (d) fourth pricing period.

TABLE 10. Optimal parameters of PID and DFOPID controllers for electrochemical process.

	Pricing periods	K_p	K_i	K_d	λ	μ
PID	$1st$	44.0760	0.6317	8.9832	-	-
	$2ed$	47.8945	0.0530	4.4522	-	-
	$3th$	29.7646	1.7019	7.8574	-	-
	$4th$	59.2594	8.6785	6.1283	-	-
DFOPID	$1st$	50.7085	57.7840	4.5929	1.1544	6.5440
	$2ed$	82.8702	98.4126	98.2195	0.8309	4.2856
	$3th$	39.8445	52.1801	0.6790	0.9938	8.1607
	$4th$	44.0694	81.0418	9.3573	1.0458	5.6397

Based on the production process and industrial data of Zhuzhou smeltery, the STA is used to solve the above optimization problem. Then, the control effects of one series of electrochemical processes in four pricing periods are selected for analysis. The system responses of the first series of processes are shown in Figs. 15-16. Furthermore, the optimal

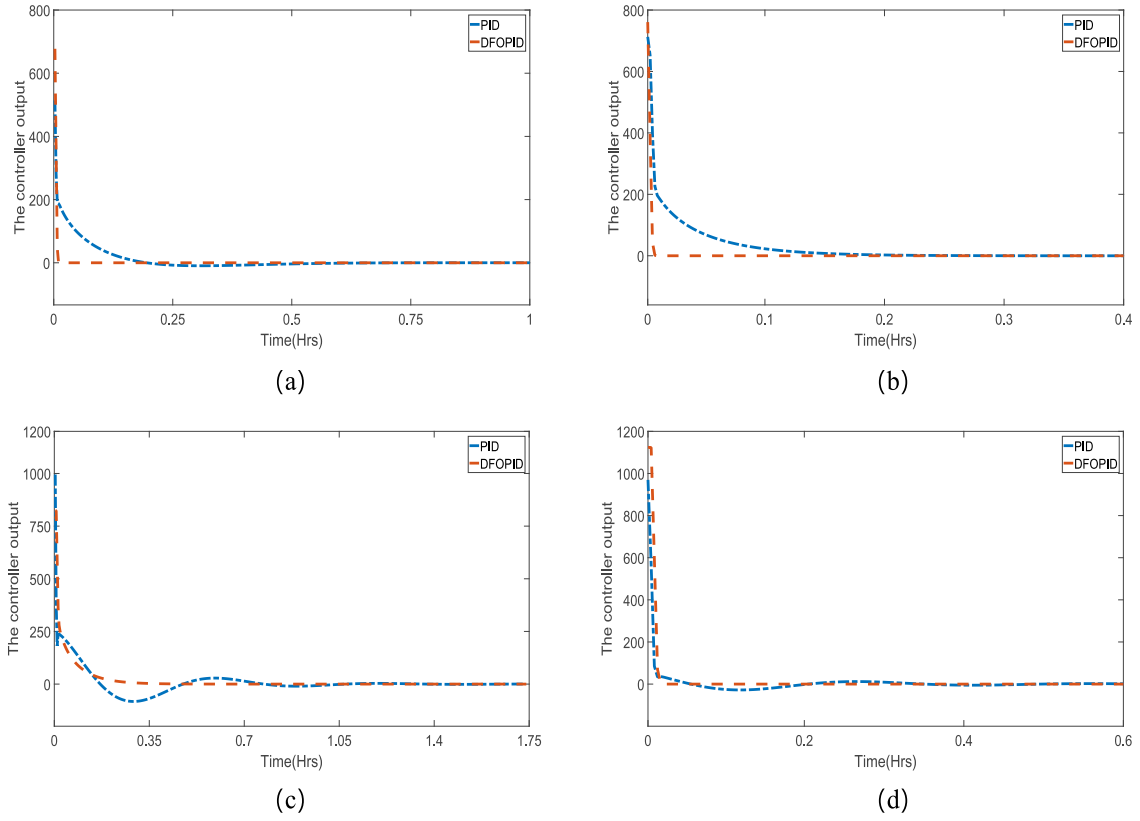

FIGURE 16. The controller output in the first series of electrochemical processes during the (a) first pricing period, (b) second pricing period, (c) third pricing period, and (d) fourth pricing period.

results are listed in Table 10. From the response curve we can conclude that the DFOPID control strategy allows the system to reach the required objective faster and consume less control energy. In addition, compared to conventional PID controlled systems, the DFOPID controlled systems have less oscillation, which is not only beneficial to the stable operation of the system, but also extends the service life of the governor mechanism.

V. CONCLUSION

In this paper, the structure of DFOPID controller are established based on the concepts of the fractional-order calculus, Tustin rule and Taylor series. Then we focus on investigating the optimal setting of the approximation function's order and five parameters for solving the stability problem in the complex industrial process. Based on the ITAE criterion, the above design problem is transformed into a nonconvex optimization problem. Next, a novel intelligent optimization search algorithm, which is named state transition algorithm, is employed to solve the this optimization problem. Applications of this method to the some practical industrial systems show that the proposed DFOPID control strategy can solve the stability problem more effectively. Furthermore, experimental results also indicate that the DFOPID control strategy leads to a better response performance and consumes less control energy when compared with conventional PID controller.

REFERENCES

[1] F. Merrikh-Bayat, S.-N. Mirebrahimi, and M. R. Khalili, "Discrete-time fractional-order PID controller: Definition, tuning, digital realization and some applications," *Int. J. Control Automat. Syst.*, vol. 13, no. 1, pp. 81–90, 2014.
[2] I. Podlubny, "Fractional-order systems and $PI^{\lambda}D^{\mu}$ controllers," *IEEE Trans. Autom. Control*, vol. 44, no. 1, pp. 208–214, Jan. 1999.
[3] Q. Gao, J. Chen, L. Wang, S. Xu, and Y. Hou, "Multiobjective optimization design of a fractional order PID controller for a gun control system," *Sci. World J.*, vol. 2013, 2013, Art. no. 907256.
[4] O. Saleem and F. Abbas, "Nonlinear self-tuning of fractional-order PID speed controller for PMDC motor," in *Proc. 13th Int. Conf. Emerg. Technol. (ICET)*, 2017, pp. 1–6.
[5] C. A. Monje, Y. Chen, B. M. Vinagre, D. Xue, and V. Feliu-Batlle, *Fractional-order Systems and Controls: Fundamentals and Applications*. London, U.K.: Springer, 2010.
[6] P. Mishra, V. Kumar, and K. Rana, "A fractional order fuzzy PID controller for binary distillation column control," *Expert Syst. Appl.*, vol. 42, no. 22, pp. 8533–8549, 2015.
[7] S. Das, I. Pan, and S. Das, "Performance comparison of optimal fractional order hybrid fuzzy PID controllers for handling oscillatory fractional order processes with dead time," *ISA Trans.*, vol. 52, no. 4, pp. 550–566, 2013.
[8] P. Ostalczyk, "Variable-, fractional-order discrete PID controllers," in *Proc. Int. Conf. Methods Models Autom. Robot.*, 2012, pp. 534–539.
[9] K. Oprzedkiewicz, "Control of an oriented PV system with the use of a discrete, robust, fractional order PID controller," *Progress in Automation, Robotics and Measuring Techniques*. Cham, Switzerland: Springer, vol. 350, 2015, pp. 177–186.
[10] P. Ostalczyk, "Stability analysis of a discrete-time system with a variable-, fractional-order controller," *Bull. Polish Acad. Sci., Tech. Sci.*, vol. 58, no. 4, pp. 613–619, 2010.

[11] K. Erenturk, "Fractional-order $PI^{\lambda}D^{\mu}$ and Active Disturbance Rejection Control of Nonlinear Two-Mass Drive System," *IEEE Trans. Ind. Electron.*, vol. 60, no. 9, pp. 3806–3813, Sep. 2013.
[12] M. A. Al-Alaoui *et al.*, "Discretization methods of fractional parallel PID controllers," in *Proc. Int. Conf. Electron., Circuits, Syst.*, 2009, pp. 327–330.
[13] A. Chakrabortty and M. Arcak, "Robust stabilization and performance recovery of nonlinear systems with unmodeled dynamics," *IEEE Trans. Autom. Control*, vol. 54, no. 6, pp. 1351–1356, Jun. 2009.
[14] R. Chai, A. Savvaris, A. Tsourdos, S. Chai, and Y. Xia, "Trajectory optimization of space maneuver vehicle using a hybrid optimal control solver," *IEEE Trans. Cybern.*, vol. 49, no. 2, pp. 467–480, Feb. 2019.
[15] L. Wu, C. Zuo, and H. Zhang, "A cloud model based fruit fly optimization algorithm," *Knowl.-Based Syst.*, vol. 89, pp. 603–617, Nov. 2015.
[16] X. Zhou, C. Yang, and W. Gui, "State transition algorithm," *J. Ind. Manage. Optim.*, vol. 8, no. 4, pp. 1039–1056, 2012.
[17] X. Zhou, D. Y. Gao, C. Yang, and W. Gui, "Discrete state transition algorithm for unconstrained integer optimization problems," *Neurocomputing*, vol. 173, pp. 864–874, Jan. 2016.
[18] X. Zhou, C. Yang, and W. Gui, "Nonlinear system identification and control using state transition algorithm," *Appl. Math. Comput.*, vol. 226, pp. 169–179, Jan. 2014.
[19] X. Zhou, J. Long, C. Xu, and G. Jia, "An external archive-based constrained state transition algorithm for optimal power dispatch," *Complexity*, vol. 2019, Jan. 2019, Art. no. 4727168.
[20] X. Zhou, C. Yang, and W. Gui, "A statistical study on parameter selection of operators in continuous state transition algorithm," *IEEE Trans. Cybern.*, to be published. doi: 10.1109/TCYB.2018.2850350.
[21] X. Zhou, D. Y. Gao, and C. Yang, "A comparative study of state transition algorithm with harmony search and artificial bee colony," in *Proc. 8th Int. Conf. Bio-Inspired Comput., Theories Appl.*, in Advances in Intelligent Systems and Computing, vol. 213, 2013, pp. 651–659.
[22] X. Zhou, P. Shi, C.-C. Lim, C. Yang, and W. Gui, "A dynamic state transition algorithm with application to sensor network localization," *Neurocomputing*, vol. 273, pp. 237–250, Jan. 2018.
[23] X. Zhou, J. Zhou, C. Yang, and W. Gui, "Set-point tracking and multi-objective optimization-based PID control for the goethite process," *IEEE Access*, vol. 6, pp. 36683–36698, 2018.
[24] Z. Huang, C. Yang, X. Zhou, and W. Gui, "A novel cognitively inspired state transition algorithm for solving the linear bi-level programming problem," *Cogn. Comput.*, vol. 10, no. 5, pp. 816–826, 2018.
[25] Z. Huang, C. Yang, X. Zhou, and T. Huang, "A hybrid feature selection method based on binary state transition algorithm and relieff," *IEEE J. Biomed. Health Inform.*, to be published. doi: 10.1109/JBHI.2018.2872811.
[26] X. Zhou, D. Y. Gao, and A. R. Simpson, "Optimal design of water distribution networks by a discrete state transition algorithm," *Eng. Optim.*, vol. 48, no. 4, pp. 603–628, 2016.
[27] Y. Wang, H. He, X. Zhou, C. Yang, and Y. Xie, "Optimization of both operating costs and energy efficiency in the alumina evaporation process by a multi-objective state transition algorithm," *Can. J. Chem. Eng.*, vol. 94, no. 1, pp. 53–65, 2016.
[28] G. Wang, C. Yang, H. Zhu, Y. Li, X. Peng, and W. Gui, "State-transition-algorithm-based resolution for overlapping linear sweep voltammetric peaks with high signal ratio," *Chemometrics Intell. Lab. Syst.*, vol. 151, pp. 61–70, Feb. 2016.
[29] F. Zhang, C. Yang, X. Zhou, and W. Gui, "Fractional-order PID controller tuning using continuous state transition algorithm," *Neural Comput. Appl.*, vol. 29, no. 10, pp. 795–804, 2018.
[30] I Petráš, "Fractional-order feedback control of a DC motor," *J. Elect. Eng.*, vol. 60, no. 3, pp. 117–128, 2009.
[31] J. J. Liang, A. K. Qin, P. N. Suganthan, and S. Baskar, "Comprehensive learning particle swarm optimizer for global optimization of multimodal functions," *IEEE Trans. Evol. Comput.*, vol. 10, no. 3, pp. 281–295, Jun. 2006.
[32] R. Chai, A. Savvaris, and A. Tsourdos, "Violation learning differential evolution-based hp-adaptive pseudospectral method for trajectory optimization of space maneuver vehicle," *IEEE Trans. Aerosp. Electron. Syst.*, vol. 53, no. 4, pp. 2031–2044, Aug. 2017.
[33] B.-S. Chen and T.-Y. Yang, "Robust optimal model matching control design for flexible manipulators," *J. Dyn. Syst., Meas., Control*, vol. 115, no. 1, pp. 173–178, 1993.
[34] Y. Wang, Z. Cai, and Q. Zhang, "Differential evolution with composite trial vector generation strategies and control parameters," *IEEE Trans. Evol. Comput.*, vol. 15, no. 1, pp. 55–66, Feb. 2011.
[35] M. Huang, X. Zhou, T. Huang, C. Yang, and W. Gui, "Dynamic optimization based on state transition algorithm for copper removal process," *Neural Computing and Applications*. Springer, 2017, pp. 1–13. doi: 10.1007/s00521-017-3232-0.
[36] J. Han, C. Yang, X. Zhou, and W. Gui, "A two-stage state transition algorithm for constrained engineering optimization problems," *Int. J. Control, Automat. Syst.*, vol. 16, no. 2, pp. 522–534, 2018.

FENGXUE ZHANG received the bachelor's degree in automation from Central South University, Changsha, China, in 2015, where she is currently pursuing the Ph.D. degree in control science and engineering. She is also a joint Ph.D. student with the University of Pittsburgh, Pittsburgh, PA, USA. Her research interests include optimization and control of industrial process, fractional order control, fuzzy control, and intelligent optimization algorithm.

CHUNHUA YANG (M'09) received the M.Eng. degree in automatic control engineering and the Ph.D. degree in control science and engineering from Central South University, China, in 1988 and 2002, respectively. She was with the Electrical Engineering Department, Katholieke Universiteit Leuven, Belgium, from 1999 to 2001. She is currently a Full Professor with the School of Information Science and Engineering, Central South University. Her research interests include modeling and optimal control of complex industrial process, intelligent control systems, and fault-tolerant computing of real-time systems.

XIAOJUN ZHOU received the bachelor's degree in automation from Central South University, Changsha, China, in 2009, and the Ph.D. degree in applied mathematics from Federation University Australia, in 2014. He is currently an Associate Professor with Central South University. His main interests include modeling, optimization and control of complex industrial process, optimization theory and algorithms, state transition algorithm, duality theory and their applications.

WEIHUA GUI (M'09) received the B.Eng. degree in automatic control engineering, and the M.Eng. degree in control science and engineering from Central South University, Changsha, China, in 1976 and 1981, respectively. From 1986 to 1988, he was a Visiting Scholar with Universitat-GH-Duisburg, Germany. He has been a Full Professor with the School of Information Science and Engineering, Central South University, since 1991. His main research interests are in modeling and optimal control of complex industrial process, distributed robust control, and fault diagnoses. He is a member of the Chinese Academy of Engineering.